Eddy-current losses in laminated and solid steel stator back iron in a small rotary brushless permanent-magnet actuator

Document Version:
Publisher's PDF, also known as Version of Record (includes final page, issue and volume numbers)

Please check the document version of this publication:

• A submitted manuscript is the version of the article upon submission and before peer-review. There can be important differences between the submitted version and the official published version of record. People interested in the research are advised to contact the author for the final version of the publication, or visit the DOI to the publisher's website.
• The final author version and the galley proof are versions of the publication after peer review.
• The final published version features the final layout of the paper including the volume, issue and page numbers.

Link to publication

Download date: 16. Nov. 2023

Eddy-Current Losses in Laminated and Solid Steel Stator Back Iron in a Small Rotary Brushless Permanent-Magnet Actuator

Johannes J. H. Paulides, Koen J. Meessen, and Elena A. Lomonova

Eindhoven University of Technology, Eindhoven 5600 MB, The Netherlands

The ever-increasing necessity to miniaturize smooth torque rotary actuators has placed severe constraints on the current slotless permanent-magnet technology. These constraints are mainly the consequence of the relatively large effective magnetic airgap which limits the achievable magnetic loading and, therefore, the torque density of slotless permanent-magnet rotary actuators. Further, the miniaturization has to be achieved at ever-decreasing costs and, therefore, it would be advantageous to implement solid back irons. However this, even at reduced magnetic loading, still results in considerable eddy-current losses. Therefore, a careful selection of the various actuator dimensions and most appropriate soft magnetic laminated or solid material is a prerequisite for applications that require smooth speed and torque characteristic. This paper will identify the influence of various parameters of the slotless permanent-magnet actuator on the eddy-current loss in the back iron using both 2-D and 3-D finite-element analysis.

Index Terms—**Actuators, brushless machines, eddy currents, iron losses, permanent magnet (PM).**

I. INTRODUCTION

THERE is a growing interest in employing small rotary slotless permanent-magnet actuators for direct-drive low-cost servo systems (i.e., demanding precision dynamic characteristics), due to their simple geometry, torque ripple reduction, and possibility for self-bearing operation [1]. Although the power density of slotless actuators may be lower than that for equivalent slotted machines, the emergence of ever higher energy permanent magnets and arrangements (e.g., Halbach) have promoted a renewed interest in slotless actuators [2].

In these slotless actuators, the winding differs from conventional machines which are inserted in the slots. For example, the windings in slotless motors can be printed-circuit coils placed in the airgap [3] or various types of surface windings fixed on the inside of the stator iron core. In general, commercial brushless ac servo motors use the rhombic winding technology, because its winding end occupies the valid axial length of the actuator and results in a sinusoidal back EMF [4]. However, the main disadvantage of the slotless topology is that it has relatively low self- and mutual-winding inductances, which influences the steady-state and transient dynamic performance.

Since industrial applications require miniaturization at low costs, one possibility is to use a solid back iron for slotless permanent-magnet (PM) actuators. However, this can result in considerable eddy-current losses which, together with the low winding inductances, compromise the dynamic performance of the slotless PM actuator. This paper, therefore, discusses the influence of using various lamination grades or solid materials as a stator back iron, for example, substituting the laminations by a solid material for a rotary actuator (Fig. 1) used for the θ axis in a commercial (X, Y, Z, and θ axes) multiaxes pick-and-place robot [5].
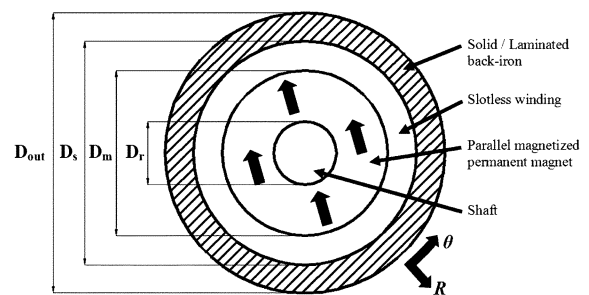
Fig. 1. Cross section of the rotary slotless actuator under investigation.

II. IRON LOSS IN SOLID BACK IRON

Numerous research efforts have been undertaken on the interaction of PMs with ferromagnetic or nonmagnetic solid back irons. As such, some authors have investigated eddy-current losses in a plate [6], [7]. Commonly, a finite-element analysis is used to investigate iron losses in solid structures, for example, a PM motor with solid armature [8]. Additionally, also finite-element model validations have been implemented (e.g., [9] describes the analysis of a setup with PMs and an aluminum rotor).

Further, also simplifications have been researched to provide a 2-D problem for a transverse flux linear motor [10]. For example, this paper describes a Fourier transformation to identify the magnetic flux density frequency analysis within each element of the meshed model. Consequently, the iron losses are calculated from the summation of the loss components in each element and the total iron loss by the summation of the iron losses in all of the elements. The same approach is currently available in the postprocessor of the commercial finite-element software package of Cedrat [11].

However, model accuracies pose a problem when thick laminations or solid back irons are used. Therefore, this paper presents the extent to which this method can be applied to the particular rotary actuator of Fig. 1, where the rotor inner diameter D_r, magnet outer diameter D_m, the stator inner diameter D_s, and the outer diameter D_{out}, are 4.0 mm, 10.5 mm, 14.2 mm, and 17.8 mm, respectively. The axial length of the actuator is 40 mm.

TABLE I
MATERIAL PROPERTIES AND IRON-LOSS COEFFICIENTS
FOR STATOR LAMINATION MATERIALS

		AI1010	M1000-100A	M800-50A	M300-35A
Thickness	mm	NA	1.00	0.50	0.35
Resistivity	Ωm	1.4×10^{-7}	3.0×10^{-7}	2.3×10^{-7}	5.0×10^{-7}
Density	kg/m³	7800	7800	7800	7650
Flux density at 10,000A/m	(T)	1.80	1.76	1.78	1.70

TABLE II
IRON AND EDDY-CURRENT LOSSES AND DAMPING
TORQUE FOR VARIOUS LAMINATION GRADES

Type	P_{Fe} (mW)	P_{eddy} (mW)	T_{eddy} (mNm)
M300-35A	52.4	2.4	0.02
M800-50A	60.6	10.6	0.08
M1000-100A	82.3	32.3	0.26

III. IRON LOSS IN LAMINATED BACK IRON

Several methodologies for calculating iron loss in electrical machines have been proposed, including the simple scaling of manufacturer's W/Kg data to a given core mass/fundamental frequency/average flux density. Lumped parameter models are where the stator is divided into a limited number of regions in which average time-varying flux density waveforms are obtained and detailed finite-element simulations and sophisticated loss models are applied on an element-by-element basis to field solutions [12], [13].

Considerable efforts have been devoted to analyze and improve the loss characteristics of laminated and solid soft magnetic materials [14]. These iron losses are a major roadblock in the effort to miniaturize low-cost slotless electrical actuators (i.e., (0.1–10 W). The motion profile of the pick-and-place application (considered for this paper) is translated into the constant average speed of 1200 r/min (20 Hz) that is used in all of the calculations.

The classical approach to model the iron losses is explained by the three well-known loss phenomena, namely, hysteresis loss, classical eddy-current loss, and the excess eddy-current loss [15] as

$$P_{\mathrm{Fe}} = P_{\mathrm{hysteresis}} + P_{\mathrm{excess}} + P_{\mathrm{eddy}}. \quad (1)$$

The iron loss in watts per meter³ is given by

$$P_{\mathrm{Fe}} = K_h \hat{B}^2 f + \frac{1}{T_p} \int_0^{T_p} \left[\frac{K_{\mathrm{exc}}}{8.67} \left(\frac{\mathrm{dB}(t)}{\mathrm{dt}} \right)^{3/2} + \frac{\sigma d^2}{12} \left(\frac{\mathrm{dB}(t)}{\mathrm{dt}} \right)^2 \right] \mathrm{dt} \quad (2)$$

where f is the fundamental frequency, d is the lamination thickness, σ is the electrical conductivity, K_h is (Ws/(T² kg)) the hysteresis coefficient, K_{exc} is (W/(T^{3/2}s^{2/3} kg)) the excess coefficient, and B is the instantaneous flux density [16]. The assumption in this model is that the rotational flux density can be taken into account by calculating the losses in each element and separately summing the loss due to the radial and tangential flux density components. It is worth noting that this model does not take the existence of any minor loop into account due to the near sinusoidal shape of the flux density waveforms in this slotless rotary actuator.

The iron-loss calculation has been undertaken for various lamination grades and thicknesses, as summarized in Table I, where Table II shows the results of the iron loss and eddy-current losses at a constant speed of 1200 r/min. This clearly shows

that the losses increase with the lamination thickness; however, the manufacturability and the cost price significantly reduce with increasing lamination thickness (REF SURA).

Most conventional laminated electrical machines are manufactured using various grades of silicon iron with a silicon content of ∼3%. In these laminations, the classical eddy-current loss is well documented with well-proven expressions for small lamination thicknesses. However, for solid materials, the aforementioned analysis cannot be used, and 3-D analysis should be undertaken, although 2-D approximation could be used as will be explained in Section IV-C.

IV. SOLID BACK-IRON EDDY-CURRENT LOSSES

The classical eddy-current loss represents the power-loss component due to the Joule effect heating of the induced eddy currents within the conducting electrical steel.

A. Semianalytical Eddy-Current Calculation

Very elegant semianalytical solutions exist to investigate the eddy currents loss in a cylindrical configuration, the solid stator back iron, with a permanent magnet (e.g., [17]). However, the main disadvantage of these methods is that they assume the stator material to be linear. Therefore, the method cannot include the case when the stator is made of a saturated ferromagnetic material; hence, for this slotless actuator, where material costs are at a premium, therefore, a finite-element software package is used to investigate the various parameter influences on the eddy-current loss [11].

B. 3-D Versus 2-D Finite-Element Analysis

Initially, a 3-D model has been prepared to calculate the eddy-current loss within the slotless motor, as shown in Fig. 2. However, some assumptions are needed for 2-D and 3-D modeling, where: 1) steady-state operation is considered; 2) the laminated and solid core assume homogeneous conducting with isotropic permeability (hence, no temperature effects); 3) iron saturation is taken into account (nonlinear BH characteristic); 4) with the 2-D analysis, end effects are neglected; hence, R θ and Z-field source and eddy-current components are orthogonal and independent of each other.

Although the eddy-current losses occur in all parts of the machine, in this model, only the eddy-current losses in the back iron are considered. For the solid stator back iron, nonlinear mild steel AI1010 is used. The permanent magnet is a NdFeB permanent magnet, with a remanent flux density of 1.2T and a relative permeability of 1.05. The electric resistivity of the material, used for the back iron, is set to a value $1.4 \times 10^{-7}\Omega$ m.

The use of 3-D finite-element analysis enables the complete investigation of the eddy currents, where even the influence of
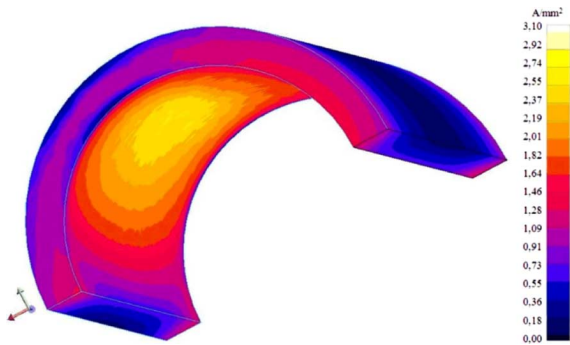
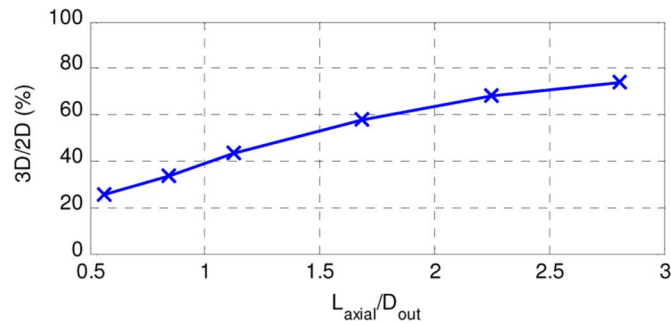Fig. 2. Eddy-current density in the slotless actuator under investigation.

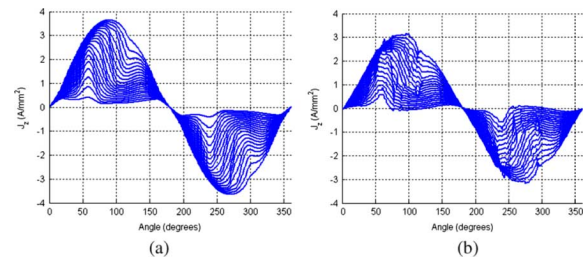Fig. 3. 3-D versus 2-D for various ratios of the axial length versus the outer diameter.

Fig. 4. Eddy-current density in the back iron of the rotary slotless actuator at various radii for (a) the 2-D analysis and (b) the 3-D analysis. The stator back iron is divided into 20 rings, where the line indicating the lowest current density represents the outer ring of the back iron, the line indicating the highest current density represents the inner ring of the back iron.
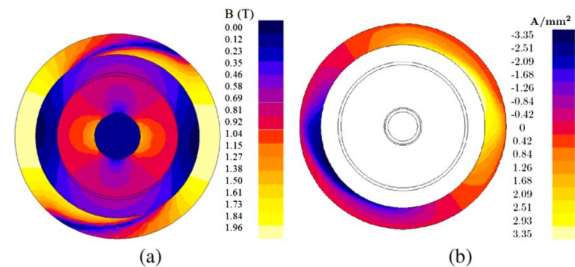

Fig. 5. (a) Distorted flux density. (b) Eddy-current density in the slotless permanent-magnet actuator (2-D FEM).

temperature effects on the material resistivity could be incorporated. However, this is very time-consuming; therefore, from a design point of view, a faster, however, less accurate, 2-D model would be favorable.

It is worth noting that many authors have initiated a correction factor in addition to the 2-D analysis to account for the end effects [18], [19] by means of analytical or empirical results. However, this research was mainly initiated for end effects on the side of the rotor within induction machines, where the dynamic behavior occurs within the rotor. In slotless machines, the dynamic effect results in the stator due to the rotating permanent-magnetic field of the rotor.

In this paper, the eddy-current loss is presented without correcting the end effects to clearly identify the limitations of the 2-D analysis. This means that instead of eddy-current loops, the induced currents are assumed to flow solely in the axial direction. This assumption is reasonable in brushless permanent-magnet machines, where the axial length is much larger than the outer diameter. Therefore, 3-D FE analysis has been undertaken which extends the ratio between axial length and diameter, providing valid modeling of the eddy currents in 2-D FE.

Clearly, from Fig. 3, it can be seen that 2-D and 3-D converge to similar values although 2-D overestimates the eddy-current losses by about 30% in the case of an axial length and outer diameter of 40 mm and 17.8 mm, respectively.

C. 2-D Implemented Finite-Element Model

All of the initial simulations used to investigate the influence of different materials on the eddy-current loss are performed at a fixed speed and the hysteresis losses and excess losses in the

back iron are calculated to be 50 mW. Further, all simulations for eddy-current losses at no load and with current applied to the windings are performed. The conclusion from these simulations is that the extra eddy-current losses caused by the applied current are negligible. Therefore, all results presented here are at no load.

To calculate the total eddy-current losses, the back iron is split into 20 rings. In each ring, the current density is assumed to be constant in the radial direction. Fig. 4 shows the current density versus angle in the rings of the back iron for (a) the 2-D and (b) 3-D finite-element analysis. The inner ring has the highest current density and the outer ring the lowest current density. The losses are calculated using the root mean square (rms) value of the current density in one ring, integrated over the surface of that ring. The current through the ring squared times the resistance of the ring gives the eddy-current loss in each ring, which is summed to provide the total eddy-current loss in the back iron. Fig. 5 illustrates (a) the flux density and (b) the induced eddy-current density in the back iron.

V. INFLUENCE OF MATERIAL RESISTIVITY

Compared to the actuator power and torque, 1.1 W and 8.7 mNm, respectively, the eddy-current losses are significant for a resistivity of 1.4×10^{-7} Ω m (i.e., a damping torque of 7.9 mNm). Using the 2-D FE analysis, Table III shows the eddy-current losses at no load for various values of resistivity for solid steel. The resistivity is increased from 1.4×10^{-7} Ω m, (mild steel or AI1010), up to 6.0×10^{-7} Ω m (REF SURA).

VI. INFLUENCE OF ACTUATOR DIAMETER

The influence of varying the outer diameter on eddy-current loss and damping torque is shown in Table IV. Considering the

TABLE III
SOLID STEEL EDDY-CURRENT LOSSES AND DAMPING TORQUE

ρ (Ωm)	P_{eddy} (mW)	T (mNm)
1.4e-7	995	7.9
2.0e-7	702	5.7
4.0e-7	340	2.7
6.0e-7	227	1.8

TABLE IV
SOLID STEEL EDDY-CURRENT LOSSES AND DAMPING
TORQUE FOR VARIOUS MOTOR OUTER DIAMETERS

D (mm)	P_{eddy} (mW)	T (mNm)
16.5	548	4.4
17.5	883	7.1
18.5	1253	10.0
19.5	1571	12.6

TABLE V
SOLID STEEL EDDY-CURRENT LOSSES AT VARIOUS SPEED RATINGS

n (rpm)	P_{eddy} (mW)	T (mNm)
400	105	2.5
600	240	3.9
800	437	5.2
1000	688	6.6
1200	995	7.9

dependency of the eddy-current loss on the frequency and the flux density, it could be concluded that increasing the outer diameter would reduce the eddy-current losses. However, the relatively small reduction in the flux density levels does not counteract the increase in iron volume. Further, reducing the outer diameter causes saturation within the back iron. Therefore, an optimum exists between the eddy-current loss and the saturation level. On the contrary, increasing the outer diameter in the laminated back iron reduces the eddy-current losses (e.g., an outer diameter of 17.8 mm and 19.5 mm provides 32.3 mW and 27.0 mW, respectively).

VII. INFLUENCE OF SPEED

To provide a complete eddy-current loss analysis, the influence of reduced speed in the actuator is also investigated. This is summarized in Table V, where a constant electric resistivity of $1.4 \times 10^{-7} \Omega$ m is considered.

VIII. CONCLUSION

In most publications, iron-loss analysis efforts are limited to making the stator back iron into thinner laminae or adding more silicon elements to steel boards in order to reduce iron loss. Although the benefits of employing higher electrical resistivity materials are indeed evident, viz. $1.4 \times 10^{-7} \Omega$ m and $6.0 \times 10^{-7} \Omega$ m give, respectively, 995-mW and 227-mW eddy-current losses, although this comes at a considerable premium in material costs.

From this paper, it can be concluded that using a solid steel back iron is not feasible unless improved steel quality is used; hence, a lamination thickness of 1.0 mm (e.g., M 1000–100 A) provides a reasonable compromise between cost and performance.

REFERENCES

[1] Z. Ren and L. S. Stephens, "Force characteristics and gain determination for a slotless self-bearing motor," *IEEE Trans. Magn.*, vol. 42, no. 7, pp. 1849–1860, Jul. 2006.

[2] S.-M. Jang, S.-H. Lee, H.-W. Cho, and S.-K. Cho, "Analysis of unbalanced force for high-speed slotless permanent magnet machine with halbach array," *IEEE Trans. Magn.*, vol. 39, no. 5, pt. 2, pp. 3265–3267, Sep. 2003.

[3] T. S. Low, M. A. Jabbar, and T. S. Tan, "Design aspects and performance of a slotless PM motor for hard disk drives," *IEEE Ind. Appl. Mag.*, vol. 3, no. 6, pp. 43–51, Nov./Dec. 1997.

[4] Y. S. Chen, Z. Q. Zhu, and D. Howe, "Slotless brushless permanent magnet machines: Influence of design parameters," *IEEE Trans. Energy Convers.*, vol. 14, no. 3, pp. 686–691, Mar. 1999.

[5] "Assembléon looks to the future," *Manuf. Eng.*, vol. 82, no. 5, pp. 4–4, 2003.

[6] G. Sironi and J. Van Hulse, "Eddy current losses in solid iron pieces under three-dimensional magnetic field," *IEEE Trans. Magn.*, vol. MAG-14, no. 5, pp. 377–379, Sep. 1978.

[7] E. J. Woods, "Eddy current losses in solid iron with DC offset," *IEEE Trans. Power App. Syst.*, vol. PAS-100, no. 5, pp. 2241–2248, May 1981.

[8] Z. J. Liu, A. Vourdas, and K. J. Binns, "Magnetic field and eddy current losses in linear and rotating permanent magnet machines with a large number of poles," *Proc. Inst. Elect. Eng., A, Sci., Meas. Technol.*, vol. 138, no. 6, pp. 289–294, 1991.

[9] E. P. Furlani, R. Wang, and H. Kusnadi, "A 3D model for computing the torque of radial couplings," *IEEE Trans. Magn.*, vol. 31, no. 5, pp. 2522–2526, Sep. 1995.

[10] J.-Y. Lee, D.-H. Kang, J.-H. Jang, and J.-P. Hong, in *Proc. 41st IAS Annu. Meeting Rapid Eddy Current Loss Calculation for Transverse Flux Linear Motor*, , 2006, vol. 1, pp. 400–406.

[11] 2D and 3D Finite Element Software Developed, LEG and CEDRAT.

[12] A. J. Moses and G. H. Shirkoohi, "Iron loss in non-oriented electrical steels under distorted flux conditions," *IEEE Trans. Magn.*, vol. MAG-23, no. 5, pp. 3127–3220, Sep. 1987.

[13] G. R. Slemon and X. Liu, "Core losses in permanent magnet motors," *IEEE Trans. Magn.*, vol. 26, no. 5, pp. 1653–1655, Sep. 1990.

[14] A. Chebak, P. Viarouge, and J. Cros, "Analytical model for design of high-speed slotless brushless machines with smc stators," *Proc. IEMDC*, vol. 1, pp. 159–164, 2007.

[15] G. Bertotti, A. Boglietti, M. Chiampi, D. Chiarabaglio, F. Fiorillo, and M. Lazzari, "An improved estimation of iron losses in electrical machines," *IEEE Trans. Magn.*, vol. 27, no. 6, pp. 5007–5009, Nov. 1991.

[16] J. J. H. Paulides, G. W. Jewell, and D. Howe, "An evaluation of alternative stator lamination materials for a high-speed, 1.5 MW, permanent magnet generator," *IEEE Trans. Magn.*, vol. 40, no. 4, pt. 2, pp. 2041–2043, Jul. 2004.

[17] M. Markovic and Y. Perriard, "An analytical determination of eddy-current losses in a configuration with a rotating permanent magnet," *IEEE Trans. Magn.*, vol. 43, no. 8, pp. 3380–3386, Aug. 2007.

[18] H. Yee, "Effects of finite length in solid-rotor induction machines," *Proc. Inst. Elect. Eng.*, vol. 118, no. 8, pp. 1025–1033, 1971.

[19] R. L. Russell and K. H. Norsworthy, "Eddy currents and wall losses in screened-rotor induction motors," *Proc. Inst. Elect. Eng.*, vol. 105A, pp. 163–175, 1958.